Renewable Energy Integration Enhancement by Exploiting Reserve Supply Capabilities of Data Centers and Cross-region Systems in Multi-region System Dispatch

Tianyu Jin, Yuke Lu, Linquan Bai, *Senior Member*, *IEEE*, Xinyu Chen, *Member*, *IEEE*, Jinyu Wen, *Member*, *IEEE*, and Yuxin Zhang

***Abstract*—As the rapid growth of renewable energy sources (RESs) with fluctuating and uncertain power generation, reserve shortages become increasingly severe, limiting the further integration of RESs and making it essential to exploit additional reserve sources. The fast-growing data centers offer significant potential to provide reserves due to their spatial and temporal dispatch flexibility. However, large quantities of jobs in the data centers have different computing requirements, making it challenging to estimate the availability of data centers for providing reserves. Meanwhile, the regional resource mix leads to uneven reserve distribution and mismatches between reserve supply and demand. The cross-region reserve supply has the capability to mitigate such mismatches as it allows different regions to provide reserve to each other. This paper enriches the reserve sources in multi-region system dispatch to enhance renewable energy integration by exploiting the reserve supply capabilities of data centers and cross-region systems. The model for available reserves of data centers is proposed via analyzing the envelope of computing constraints of aggregated jobs. In addition, a comprehensive cross-region reserve supply model is presented by considering reserve supply and demand limitations and reserve transmission capability. Case studies are performed and the results show that the data centers can provide a substantial amount of reserves. Both the migration of jobs among data centers and the cross-region reserve supply transfer reserve resources among multiple regions. Simulations on a real-world power grid system further demonstrate that unlocking the reserve supply potential of data centers can reduce operating costs by 0.4% and the curtailment of RESs by 1.7%.**

***Index Terms*—Renewable energy source (RES), multi-region system, dispatch, flexibility, data center, cross-region reserve.**

Manuscript received: April 7, 2025; revised: August 27, 2025; accepted: December 1, 2025. Date of CrossCheck: December 1, 2025. Date of online publication: February 11, 2026.

The work of T. Jin, X. Chen, J. Wen, and Y. Zhang was partially supported by the National Science Fund for Distinguished Young Scholars of China (No. 72325006), the Basic Science Center Program of National Natural Science Foundation of China (No. 72488101), and the Major Program of National Natural Science Foundation of China (No. 72293601).

T. Jin, X. Chen, J. Wen, and Y. Zhang are with the State Key Laboratory of Advanced Electromagnetic Technology, Huazhong University of Science and Technology, Wuhan 430074, China, and T. Jin is also with William States Lee College of Engineering, University of North Carolina at Charlotte, Charlotte, NC 28223, USA (e-mail: tianyujin97@gmail.com; xchen2019@hust.edu.cn; jinyu.wen@hust.edu.cn; zyx20@hust.edu.cn).

Y. Lu is with the Institute of New Energy, Wuhan 430073, China (e-mail: 2506732061@qq.com).

L. Bai (corresponding author) is with William States Lee College of Engineering, University of North Carolina at Charlotte, Charlotte, NC 28223, USA (e-mail: linquanbai@charlotte.edu).

DOI: 10.35833/MPCE.2025.000306

NOMENCLATURE

$\lambda_{r,t}$	Proportion of servers of the r^{th} data center in off state at time t
μ_r	Computing rate of servers in the r^{th} data center
η^{tl}	Proportion of power transmission loss
$\eta_r^{es,c}$, $\eta_r^{es,d}$	Charging and discharging efficiencies of energy storage in region r
$\Delta nj_{r,t}^{-}$, $\Delta nj_{r,t}^{+}$	Reduced and increased numbers of computational jobs in the r^{th} data center at time t
Δt	Time interval
$\Delta p_{r,t}^{es,d,\max}$, $\Delta p_{r,t}^{es,c,\max}$	The maximum and minimum available discharging power of energy storage in region r at time t
$c_{k,r}^{tu}$	Unit fuel consumption of the k^{th} thermal unit in region r
$DT_{r,\tau}^{d}$	Allowed deferrable computing period of certain deferrable jobs dispatched to the r^{th} data center at time τ
$F_{k,r}^{re,up}$	Factor of upward reserve provided by the k^{th} type of renewable energy sources (RESs) in region r
$IJ_{r,\tau}^{d}$	Binary variable representing whether deferrable jobs dispatched to the r^{th} data center at time τ are required to be computed
$I_{r',r}^{tl}$, $I_{r,r'}^{tl}$	Binary variables representing directions of power transmissions between regions r' and r and between regions r and r'
$I_{k,r,t}^{tu}$	Binary operational status of the k^{th} thermal unit in region r at time t
N_{tu}, N_{re}	Numbers of thermal units and RESs

$NJ^u_{r,t}$, $NJ^d_{r,t}$ Numbers of non-deferrable and deferrable jobs dispatched to the r^{th} data center at time t

NJ^u_t, NJ^d_t Numbers of non-deferrable and deferrable jobs scheduled by cloud service provider at time t

NS_r Number of available servers of the r^{th} data centers

$Nj_{r,t}$ Accumulated number of computational jobs in the r^{th} data center by time t

$ND_{r,t}$, $NA_{r,t}$ The minimum and maximum numbers of jobs that should be computed in the r^{th} data center at time t

NR, N_{tu}, N_{re} Numbers of regions, thermal units, and RESs

$ns^{peak}_{r,t}$, $ns^{idle}_{r,t}$, $ns^{off}_{r,t}$ Numbers of servers owned by the r^{th} data center in peak, idle, and off states at time t

$nj_{r,t}$ Total number of jobs computed by the r^{th} data center at time t

P^{peak}_r, P^{idle}_r Power demands of each server of the r^{th} data center working in peak and idle states

$P^{re}_{k,r}$ Installed capacity of the k^{th} type of RESs in region r

$P^{tl}_{r',r}$, $P^{tl}_{r,r'}$ Transmission capacities between regions r' and r and between regions r and r'

$P^{tu}_{k,r}$, $\underline{P}^{tu}_{k,r}$ Installed capacity and the minimum power generation of the k^{th} thermal unit in region r

PUE_r Energy efficiency of the r^{th} data center

$P^{basic}_{r,t}$ Basic power load of region r at time t

$p^{tl}_{r',r,t}$, $p^{tl}_{r,r',t}$ Transmitted power from regions r' to r and from regions r to r' through tie lines at time t

$p^{tu}_{k,r,t}$ Power output of the k^{th} thermal unit in region r at time t

$p^{DC,se}_{r,t}$ Power demand of servers of the r^{th} data center at time t

$p^{DC}_{r,t}$ Total power demand of the r^{th} data center at time t

$p^{es,c}_{r,t}$, $p^{es,d}_{r,t}$ Charging and discharging power of energy storage in region r at time t

$p^{es,c,\max}_r$, $p^{es,d,\max}_r$ The maximum charging and discharging power of energy storage in region r

$p^{re}_{k,r,t}$ Actual power output of the k^{th} type of RESs in region r at time t

$\bar{p}^{re}_{k,r,t}$, $cf^{re}_{k,r,t}$ The maximum available power output and capacity factor of the k^{th} type of RESs in region r at time t

$R^{tu,u}_{k,r}$, $R^{tu,d}_{k,r}$ Ramp-up and ramp-down limits of the k^{th} thermal unit in region r

Res^+_r, Res^-_r Rates of upward and downward reserve of region r

$res^{+,sel}_{r,t}$, $res^{-,sel}_{r,t}$ Upward and downward reserve supplies of region r at time t

$res^{+,oth}_{r',r,t}$, $res^{-,oth}_{r',r,t}$ Upward and downward reserve productions from regions r' to r at time t

$res^{+,oth,avi}_{r,r',t}$, $res^{-,oth,avi}_{r,r',t}$ Available upward and downward reserves supplied to region r' by region r at time t

$res^{tu,+}_{k,r,t}$, $res^{tu,-}_{k,r,t}$ Upward and downward reserves that the k^{th} thermal unit in region r can supply at time t

$res^{DC,+}_{r,t}$, $res^{DC,-}_{r,t}$ Upward and downward reserves that the r^{th} data center can supply at time t

$res^{es,+}_{r,t}$, $res^{es,-}_{r,t}$ Upward and downward reserves that energy storage in region r can supply at time t

$res^{re,+}_{k,r,t}$, $res^{re,-}_{k,r,t}$ Upward and downward reserve that the k^{th} type of RESs in region r can supply at time t

$SE^{es,\min}_r$, $SE^{es,\max}_r$ The minimum and maximum levels of stored energy of energy storage in region r

$se^{es}_{r,t}$, $se^{es}_{r,t_{end}}$, se^{es}_{r,t_0} Stored energy of energy storage in region r at time t, t_{end}, and t_0

t_{start}, t_{end} Start and end time of system dispatch

I. Introduction

In recent years, China's renewable energy generation capacity has experienced significant growth [1], [2]. By the end of 2023, the installed capacities of wind and photovoltaic (PV) in China reached 441 GW and 609 GW, respectively, accounting for 15.1% and 20.9% of the national power generation capacity [3].

Reserve capacity serves as backup power generation during unexpected events and is essential to the power system [4]. Conventional thermal units and energy storage systems are the main reserve supply sources. However, as renewable energy integration grows, thermal unit generation capacity is increasingly replaced, which may lead to considerable reserve shortages. Meanwhile, the variability and uncertainty of renewable energy generation further pose challenges to reserve capacity, particularly under high renewable energy penetration [5], [6]. The increasingly severe reserve shortages impose significant barriers to large-scale renewable energy integration. Therefore, exploiting potential reserve supply sources is essential.

Geo-distributed data centers, which provide internet-scale computing services [7], [8], possess flexible scheduling capabilities. Moreover, the rapid development of large language models in recent years has significantly increased the demand for computing power, resulting in higher power consumption in data centers. In 2022, 270 TWh of electricity was consumed by the data centers in China, accounting for approximately 3% of the national electricity consumption. By 2025, 5% of China's annual electricity demand is expected to be consumed by data centers [9].

Given the significant spatial and temporal dispatch flexibility and the rapid growth in electricity consumption, data centers are viable potential reserve capacity providers to address reserve shortages caused by the increasing penetration of renewable energy sources (RESs). However, numerous computational jobs own diverse characteristics, making it challenging to estimate the reserve supply capacity of data centers while satisfying the operational constraints of individual computational jobs.

Additionally, variations in power generation capacity mix across regions lead to variations in reserve availability. This spatial imbalance may bring reserve mismatches, where the supply and demand of reserves are not aligned at the regional level.

To address this issue, cross-region reserve supply emerges as a promising solution, enabling the sharing and coordinated dispatch of reserve sources among multiple areas. By leveraging surplus flexibility in one region to support reserve demands in another, the overall system reliability can be enhanced.

However, implementing cross-region reserve supply poses several challenges. Due to the variability of available surplus reserve in each region, accurately estimating both the local reserve demands and the reserve supply capabilities becomes complex. In addition, cross-region reserve supply will take up part of the available inter-regional transmission capacity. Therefore, transmission constraints must be carefully considered when designing coordinated reserve sharing mechanisms.

Data center participation in demand response has been studied in [10]-[17]. Internet data centers are considered to exhibit demand response characteristics by offering both temporal and spatial load regulation capabilities [10], [11]. The spatial and temporal flexibilities of data centers, along with the battery energy storage systems, are utilized to optimize distribution network operation [12]. By exploring the willingness to pay and time sensitivities of data center users, the user-side demand response is devised in [13]. Reference [14] proposes an adaptive policy with quality-of-service assurance, enabling data centers to participate in regulation service programs while maintaining job service quality. Reference [15] develops a synergistic control strategy for information technology and cooling systems, allowing data centers to provide frequency regulation by tracking the regulation signal on the electricity market. The uninterruptible power supply storage systems, heating, ventilation, and air conditioning cooling units, and off-gridding ability are exploited in [16] for data centers to deliver fast frequency response services. In [17], a two-stage generation and transmission expansion planning framework considering the demand response of data centers is proposed. Although there is a large amount of literature on the demand response of data centers, limited research has focused on data centers providing reserve capability [18]-[21]. Reference [18] studies the optimal sizing of battery energy storage systems in data centers for offering frequency containment reserve services to the grid. Data centers are allowed to provide regulation service reserves by modeling the job processing quality of service constraints [19]. An energy- and quality-of-service-aware regulation service reserve supply approach is proposed by [20], incorporating bidding strategies and runtime policies. Large-scale flexible loads are aggregated and dispatched by data centers to supply operating reserves in the power-communication coupling networks [21]. However, the previous literature either assumes backup energy storage as the primary reserve source or introduces reserve capacity through general operational constraints of data centers. Without explicitly analyzing and modeling the computing characteristics of diverse jobs, these approaches fail to fully capture the reserve supply potential of data centers and further accurately quantify their available reserve supply capacity.

Numerous studies have been conducted on the optimal dispatch of multi-area systems under reserve constraints [22]-[32]. A multi-area dynamic economic dispatch problem with spinning reserve constraints is proposed in [22] to address hourly load variations. References [23] and [24] optimize the scheduling of multi-area integrated electricity and natural gas systems with reserve constraints. However, in the aforementioned studies, reserve demands are satisfied within each respective area, and cross-region reserve sharing is not considered. In [25], a deterministic security-constrained unit commitment model for power systems with large-scale wind power integration is developed to determine the spinning reserve requirements, optimize generator scheduling, and coordinate reserve allocation across regions. Reference [26] optimizes reserve allocation for multi-area interconnected power systems considering reserve sharing among areas, improving the consumption of wind power. In [27] and [28], a generation-reserve co-optimization dispatch model that considers the operational constraints of tie lines is proposed, which can allocate reserve sources for all areas. Reference [29] addresses the dimensioning frequency restoration reserves through a chance-constrained approach and enables reserve sharing while considering the uncertainties arising from imbalances, contingencies, and available transmission capacity. In [30] and [31], a tie-line-based energy and reserve allocation model for multi-area systems is developed, effectively relieving the energy and reserve shortages in several areas. Reference [32] proposes a dynamic reserve demand estimation model and a reserve allocation strategy for the multi-area system, ensuring overall system reliability. However, these studies primarily focus on conventional thermal units as reserve providers, while overlooking the flexible reserve potential of emerging sources such as data centers and energy storage. Furthermore, the available reserve capacity model is often simplified, failing to capture the complexity of spatial reserve mismatches and limiting the accurate estimation of the reserve allocation between local region and other regions.

This paper enhances renewable energy integration in multi-region system dispatch by enriching the reserve sources, with a special focus on the reserves supplied by data centers and cross-region systems. We start with the basic operating models of data centers. By aggregating computational jobs with various characteristics, we then construct an envelope of computing constraints of aggregated jobs and propose the reserve supply model of data centers. Next, we model the constraints of thermal units, energy storage, and RESs, as well as several system-level operational limits and the objective function. Particularly, regional reserve constraints are formulated by considering local flexibility and cross-region reserve scheduling. Finally, we develop a multi-region test system to examine the models of reserves supplied by data centers and cross-region systems. We also introduce a real-world power grid system to validate the proposed models. The operating cost of the whole system decreases and the renewable energy integration is improved when incorporating additional reserve sources.

The main contributions of this paper are summarized as follows.

1) We propose a novel reserve supply model for data centers based on the envelope of computing constraints derived from aggregated jobs. Unlike previous studies that only impose simplified operational constraints of data centers, this model explicitly explores and incorporates job-specific flexibility, enabling accurate estimation of reserve availability of data centers without violating the computing constraints of jobs with different computational features.

2) We formulate a comprehensive cross-region reserve supply model that integrates local reserve demands, reserve transmission limits, and various reserve sources, including thermal units, RESs, energy storage, and data centers. This model jointly optimizes both local and cross-region reserves, coordinating the dispatch of multiple reserve sources across different regions and mitigating regional reserve mismatches.

3) We design a test system interconnected by optical fibers and tie lines. The simulation results show that the reserve sources are enriched by exploiting the reserve supply capabilities of data centers and cross-region systems. The renewable energy integration is improved and the fuel consumption of thermal units with high marginal cost is reduced. In addition, we also conduct simulations on a real-world power grid system, further demonstrating that unlocking the reserve supply potential of data centers can reduce operating costs and carbon emissions.

The rest of this paper is organized as follows. The operating and reserve supply models of data centers are proposed in Section II. Section III formulates the comprehensive cross-region reserve supply model considering the reserves supplied by both data centers and cross-region systems. The case study is presented in Section IV. Section V concludes the paper.

II. Operating and Reserve Supply Models of Data Centers

In this section, we firstly provide an overview of data centers and outline several key assumptions. Next, we present the basic operating models of data centers. The constraints of computing deferrable jobs are illustrated and modeled in detail. The formulation of reserves supplied by data centers is then presented.

A. Overview and Assumptions of Data Centers

Data centers mainly consist of servers, energy storage, networking equipment, cooling systems, and other supporting devices, which are operated and managed by cloud service providers to execute a wide range of computational jobs. These jobs are generally classified into two categories: non-deferrable and deferrable [33]. Non-deferrable jobs such as real-time stock trading and earthquake warning are highly latency-sensitive and must be computed immediately upon arrival. In contrast, deferrable jobs such as machine learning model training and log analysis can tolerate certain delays in computation within a specific time window. By fully leveraging the operational flexibility, data centers can serve as valuable dispatch sources for power systems, particularly in providing reserves.

To enable efficient modeling while preserving the essential features of data center operation, the following assumptions are made.

1) All geo-distributed data centers are connected with each other by fibers and are coordinated by the cloud service provider. The communication capacity among data centers and between data centers and the cloud service provider is sufficient, ensuring timely and reliable information exchange.

2) Job is treated as the smallest computational unit and is assumed to be independent. Certain jobs can be migrated among interconnected data centers through fiber networks. When scheduling and computing jobs, the computing constraints must be satisfied to avoid potential penalties such as degradation of end-user satisfaction.

3) The cloud service provider forecasts the number and flexibility of jobs on the day-ahead time scale and then submits dispatchable computing boundaries to the power system operator, enabling coordinated operation between data centers and the power system.

B. Basic Operating Models of Data Centers

We assume the r^{th} data center located in region $r \in NR$ is dispatched by the same cloud service provider.

The total number of non-deferrable and deferrable jobs dispatched to all the data centers should match the schedules determined by the cloud service provider, respectively:

$$\begin{cases} \sum_{r=1}^{NR} NJ_{r,t}^{u} = NJ_{t}^{u} \\ \sum_{r=1}^{NR} NJ_{r,t}^{d} = NJ_{t}^{d} \end{cases} \tag{1}$$

For each server, we assume that peak, idle, and off are the three states. The total number of servers in all states should equal the number of available servers of the data centers. Meanwhile, the proportion of servers in off state is limited:

$$ns_{r,t}^{peak} + ns_{r,t}^{idle} + ns_{r,t}^{off} = NS_r \tag{2}$$

$$ns_{r,t}^{off} \le \lambda_{r,t} \cdot NS_r \tag{3}$$

The power demand of servers of the data centers is determined by both the number of servers in peak and idle states and their respective power consumption:

$$p_{r,t}^{DC,se} = ns_{r,t}^{peak} \cdot P_r^{peak} + ns_{r,t}^{idle} \cdot P_r^{idle} \tag{4}$$

Based on the power demand of servers, the total power consumption of the data centers can be modeled by incorporating the energy efficiency:

$$p_{r,t}^{DC} = PUE_r \cdot p_{r,t}^{DC,se} \tag{5}$$

The number of servers in peak state is determined by the number of computational jobs and the computing rate of each server:

$$ns_{r,t}^{peak} = \frac{nj_{r,t}}{\mu_r} \tag{6}$$

The accumulated number of computational jobs at time t is updated by the number of computational jobs at time t, and is constrained by both the minimum and maximum numbers of jobs that should be computed by time t:

$$Nj_{r,t}=Nj_{r,t-1}+nj_{r,t} \tag{7}$$

$$ND_{r,t}\le Nj_{r,t}\le NA_{r,t} \tag{8}$$

The minimum and maximum numbers of jobs that should be computed by time t are determined by the numbers of non-deferrable and deferrable jobs and the allowed deferrable computing periods of certain deferrable jobs:

$$ND_{r,t}=\sum_{\tau=1}^{t}\left(IJ_{r,\tau}^{d}\cdot NJ_{r,\tau}^{d}+NJ_{r,\tau}^{u}\right) \tag{9}$$

$$NA_{r,t}=\sum_{\tau=1}^{t}\left(NJ_{r,\tau}^{d}+NJ_{r,\tau}^{u}\right) \tag{10}$$

$$IJ_{r,\tau}^{d}=\begin{cases}1 & \tau+DT_{r,\tau}^{d}\le t\\ 0 & \tau+DT_{r,\tau}^{d}>t\end{cases} \tag{11}$$

For non-deferrable jobs, the deferrable computing periods can be assumed as zero. Constraint (8) is illustrated in Fig. 1(a).

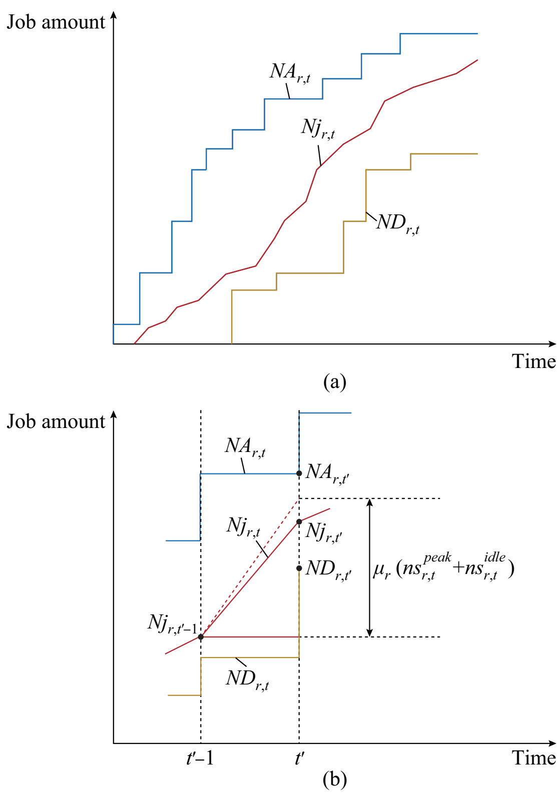

Fig. 1. Envelope of computing constraints of aggregated jobs presented in general and in detail. (a) In general. (b) In detail.

The above formulations describe the basic operating models of data centers. Similar models have been employed in existing studies [19], [20] to investigate the reserve supply capabilities of data centers. However, these models merely offer an abstract representation of the reserve potential of data centers and lack a quantitative assessment of their actual reserve supply capabilities.

To bridge this gap, we propose the reserve supply model of data centers based on the envelope of computing constraints of aggregated jobs in the following subsection.

C. Formulation of Reserves Supplied by Data Centers

Due to the deferred computing characteristics of deferrable tasks, $Nj_{r,t}$ in Fig. 1(a) can be regulated, which further influences the load profile of data centers. Since the number of computational jobs scheduled for the next time interval can be flexibly adjusted, data centers are enabled to supply both upward and downward reserves.

Figure 1(b) presents a zoom-in view of Fig. 1(a) from time $t'-1$ to t', where the red dashed line indicates the adjustable range. By analyzing the detailed envelope of computing constraints of aggregated jobs, the reserve supplied by the data centers is modeled.

Given the originally scheduled $Nj_{r,t}$, a reduction in the number of computational jobs at time t leads to a lower power demand for the data centers, indicating the capability of such data centers to provide upward reserve $res_{r,t}^{DC,+}$ for the power system:

$$res_{r,t}^{DC,+}=\frac{\Delta nj_{r,t}^{-}}{\mu_r}\left(P_r^{peak}-P_r^{idle}\right) \tag{12}$$

Constrained by (8), the reduced accumulated number of computational jobs should also be limited by $ND_{r,t}$. Therefore, $\Delta nj_{r,t}^{-}$ should be constrained by:

$$nj_{r,t}-\Delta nj_{r,t}^{-}=\max\left(ND_{r,t}-Nj_{r,t-1},0\right) \tag{13}$$

Similarly, given the originally scheduled $Nj_{r,t}$, an increase in the number of computational jobs at time t results in a higher power demand for the data centers, implying the capability of such data centers to provide downward reserve $res_{r,t}^{DC,-}$ for the power system:

$$res_{r,t}^{IDC,-}=\frac{\Delta nj_{r,t}^{+}}{\mu_r}\left(P_r^{peak}-P_r^{idle}\right) \tag{14}$$

Constrained by (8), the increased accumulated number of computational jobs should also be limited by $NA_{r,t}$. In addition, the maximum available computing capability of the data centers should always be considered. Therefore, $\Delta nj_{r,t}^{+}$ is determined by:

$$nj_{r,t}+\Delta nj_{r,t}^{+}=\min\left(NA_{r,t}-Nj_{r,t-1},\mu_r\left(ns_{r,t}^{peak}+ns_{r,t}^{idle}\right)\right) \tag{15}$$

III. Comprehensive Cross-Region Reserve Supply Model Considering Reserves Supplied by Both Data Centers and Cross-Region Systems

In this section, we firstly model the operational constraints of thermal units, energy storage, and RESs. Next, regional power balance constraints and regional reserve constraints considering cross-region reserve supply are presented. Finally, the objective function is given.

A. Thermal Units

The power output of the thermal unit is limited by operational status, installed capacity, and the minimum power generation:

$$I_{k,r,t}^{tu}\underline{P}_{k,r}^{tu} \leq p_{k,r,t}^{tu} \leq I_{k,r,t}^{tu}P_{k,r}^{tu} \tag{16}$$

The ramping rates should not exceed the ramp-up and ramp-down limits:

$$p_{k,r,t}^{tu}-p_{k,r,t-1}^{tu} \leq R_{k,r}^{tu,u} \tag{17}$$

$$p_{k,r,t-1}^{tu}-p_{k,r,t}^{tu} \leq R_{k,r}^{tu,d} \tag{18}$$

The upward reserve provided by the thermal unit is limited by operational status, installed capacity, power generation, and ramp limits, while the downward reserve is constrained by operational status, the minimum power generation, and ramp limits:

$$res_{k,r,t}^{tu,+}=\min\left(I_{k,r,t}^{tu}P_{k,r}^{tu}-p_{k,r,t}^{tu}, R_{k,r}^{tu,u}-p_{k,r,t}^{tu}+p_{k,r,t-1}^{tu}\right) \tag{19}$$

$$res_{k,r,t}^{tu,-}=\min\left(p_{k,r,t}^{tu}-I_{k,r,t}^{tu}\underline{P}_{k,r}^{tu}, R_{k,r}^{tu,d}-p_{k,r,t-1}^{tu}+p_{k,r,t}^{tu}\right) \tag{20}$$

B. Energy Storage

The charging and discharging power of the energy storage should not exceed the maximum charging and discharging power limits, respectively:

$$\begin{cases} 0 \leq p_{r,t}^{es,c} \leq p_r^{es,c,\max} \\ 0 \leq p_{r,t}^{es,d} \leq p_r^{es,d,\max} \end{cases} \tag{21}$$

The stored energy of the energy storage at time t is updated by the stored energy at time $t-\Delta t$, charging and discharging power, and charging and discharging efficiency:

$$se_{r,t}^{es}=se_{r,t-\Delta t}^{es}+\left(\eta_r^{es,c}p_{r,t}^{es,c}-\frac{p_{r,t}^{es,d}}{\eta_r^{es,d}}\right)\Delta t \tag{22}$$

Meanwhile, the stored energy of the energy storage is constrained by the minimum and maximum levels of stored energy:

$$SE_r^{es,\min} \leq se_{r,t}^{es} \leq SE_r^{es,\max} \tag{23}$$

The terminal stored energy should equal the initial stored energy:

$$se_{r,t_0}^{es}=se_{r,t_{end}}^{es} \tag{24}$$

The upward reserve provided by energy storage is determined by the maximum available discharging power, the maximum discharging power, and the charging and discharging power:

$$res_{r,t}^{es,+}=\min\left(\Delta p_{r,t}^{es,d,\max}, p_r^{es,d,\max}\right)-p_{r,t}^{es,d}+p_{r,t}^{es,c} \tag{25}$$

The maximum available discharging power of the energy storage is constrained by the minimum stored energy level and the stored energy at time $t-\Delta t$:

$$\Delta p_{r,t}^{es,d,\max}=\frac{\left(se_{r,t-\Delta t}^{es}-SE_r^{es,\min}\right)\eta_r^d}{\Delta t} \tag{26}$$

Similarly, the downward reserve provided by energy storage is determined by the maximum available charging power, the maximum charging power, and the charging and discharging power:

$$res_{r,t}^{es,-}=\min\left(\Delta p_{r,t}^{es,c,\max}, p_r^{es,c,\max}\right)+p_{r,t}^{es,d}-p_{r,t}^{es,c} \tag{27}$$

The maximum available charging power of the energy storage is constrained by the maximum stored energy level and the stored energy at time $t-\Delta t$:

$$\Delta p_{r,t}^{es,c,\max}=\frac{SE_r^{es,\max}-se_{r,t-\Delta t}^{es}}{\eta_r^c\Delta t} \tag{28}$$

C. RESs

The actual power output of RESs should not exceed the maximum available power generation, which is determined by both the capacity factor and installed capacity:

$$0 \leq p_{k,r,t}^{re} \leq \bar{p}_{k,r,t}^{re} \tag{29}$$

$$\bar{p}_{k,r,t}^{re}=cf_{k,r,t}^{re} \cdot P_{k,r}^{re} \tag{30}$$

The upward reserve provided by RESs is constrained by the factor of upward reserve of RESs, the maximum available power generation, and the actual power output, while the downward reserve is determined by the actual power output:

$$res_{k,r,t}^{re,+}=F_{k,r}^{re,up}\bar{p}_{k,r,t}^{re}-p_{k,r,t}^{re} \tag{31}$$

$$res_{k,r,t}^{re,-}=p_{k,r,t}^{re} \tag{32}$$

D. Regional Power Balance Constraints

In region r, the power demand is balanced by thermal units, energy storage, RESs, and power transmission by cross-region tie lines. The power balance constraints can be expressed as:

$$\sum_{k=1}^{Ntu}p_{k,r,t}^{tu}+p_{r,t}^{es,d}-p_{r,t}^{es,c}+\sum_{k=1}^{Nre}p_{k,r,t}^{re}+\sum_{r'=1}^{NR}\left(\eta^{tl}p_{r',r,t}^{tl}-p_{r,r',t}^{tl}\right)= p_{r,t}^{DC}+P_{r,t}^{basic} \quad r' \neq r \tag{33}$$

The transmitted power between regions r' and r is constrained by the direction of power transmission and the transmission capacity of tie lines:

$$\begin{cases} 0 \leq p_{r',r,t}^{tl} \leq I_{r',r}^{tl}P_{r',r}^{tl} \\ 0 \leq p_{r,r',t}^{tl} \leq I_{r,r'}^{tl}P_{r,r'}^{tl} \end{cases} \tag{34}$$

$$I_{r',r}^{tl}+I_{r,r'}^{tl}=1 \tag{35}$$

$$P_{r',r}^{tl}=P_{r,r'}^{tl} \tag{36}$$

E. Regional Reserve Constraints

Both the reserve supply and demand limit the capability of cross-region reserve supply. In regions r, the reserve requirement is satisfied by both local and cross-region reserve supply:

$$Res_r^+ \cdot \left(p_{r,t}^{DC}+P_{r,t}^{basic}\right) \leq res_{r,t}^{+,sel}+\eta^{tl}\sum_{r'=1}^{NR}res_{r',r,t}^{+,oth} \quad r' \neq r \tag{37}$$

$$Res_r^- \cdot \left(p_{r,t}^{DC}+P_{r,t}^{basic}\right) \leq res_{r,t}^{-,sel}+\eta^{tl}\sum_{r'=1}^{NR}res_{r',r,t}^{-,oth} \quad r' \neq r \tag{38}$$

For region r, the sum of local reserve and reserve dispatched to support other regions should be equal to the reserve supplied by data centers, thermal units, energy storage, and RESs:

$$res_{r,t}^{+,sel}+\sum_{r'(r' \neq r)}^{NR}res_{r,r',t}^{+,oth,avi}=res_{r,t}^{DC,+}+\sum_{k=1}^{Ntu}res_{k,r,t}^{tu,+}+res_{r,t}^{es,+}+\sum_{k=1}^{Nre}res_{k,r,t}^{re,+} \tag{39}$$

$$res_{r,t}^{-,sel}+\sum_{r'(r'\neq r)}^{NR}res_{r,r',t}^{-,oth,avi}=res_{r,t}^{DC,-}+\sum_{k=1}^{Ntu}res_{k,r,t}^{tu,-}+res_{r,t}^{es,-}+\sum_{k=1}^{Nre}res_{k,r,t}^{re,-} \tag{40}$$

The actual cross-region reserve supply is limited by both available reserve supply from other regions and the reserve transmission capability. The latter is determined by the capacity and the transmitted power of tie lines between regions r and r'.

$$res_{r,r',t}^{+,oth}=\min\left(res_{r,r',t}^{+,oth,avi},P_{r,r'}^{tl}-p_{r,r',t}^{tl}\right) \tag{41}$$

$$res_{r,r',t}^{-,oth}=\min\left(res_{r,r',t}^{-,oth,avi},p_{r,r',t}^{tl}\right) \tag{42}$$

F. Objective Function

In this paper, the comprehensive model is designed to minimize the fuel consumption of thermal units:

$$\min\sum_{t=t_{start}}^{t_{end}}\sum_{k=1}^{Ntu}c_{k,r}^{tu}p_{k,r,t}^{tu} \tag{43}$$

IV. Case Study

In this section, we conduct several simulations on both the designed test system and a real-world power grid system. The proposed reserve supply models could enhance renewable energy consumption and reduce operating costs of these systems.

A. Test System and Scenarios

1) Test System

As shown in Fig. 2, a three-region test system is constructed. Two types of thermal units, i. e., type-a and type-b, are considered. Type-a thermal units have lower marginal costs, while type-b thermal units have shorter minimum start-up and shut-down time.

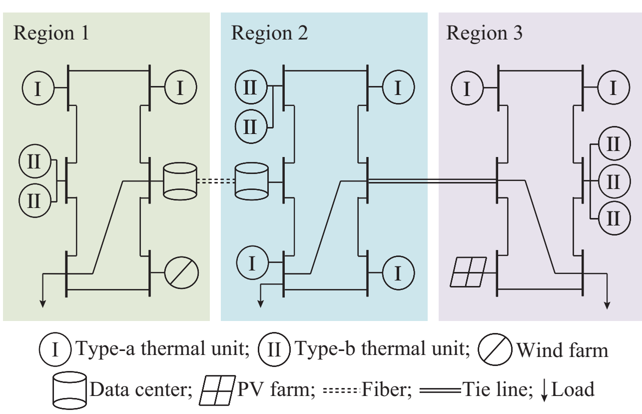

Fig. 2. Structure of three-region test system.

In Region 1, two 229 MW type-a thermal units, two 50 MW type-b thermal units, a wind farm, and data centers (DC_1) are installed. Region 2 consists of three 240 MW type-a thermal units, two 50 MW type-b thermal units, and data centers (DC_2). Two 200 MW type-a thermal units, three 50 MW type-b thermal units, and a PV farm are located in Region 3. The data centers in Regions 1 and 2 are owned and dispatched by the same cloud service provider, enabling job migration between DC_1 and DC_2 through optical fibers. A 200 MW tie line is built to exchange electricity between Regions 2 and 3.

The basic load profiles of Regions 1, 2, and 3, as well as the capacity factor of PV and wind farms, are shown in Fig. 3(a) [34], [35]. The PV and wind power penetrations, defined as the ratio of the sum of power generation of RESs to the total regional power demand, are set to be 36% and 22%, respectively. In Fig. 3(b), the numbers of non-deferrable jobs NJ_t^u and deferrable jobs NJ_t^d and the minimum accumulated number of computational deferrable jobs ND_t are presented [36]. A total of 7×10^5 servers are equipped in DC_2, which is 1.75 times than that in DC_1. $\lambda_{r,t}$ is set to be 0%.

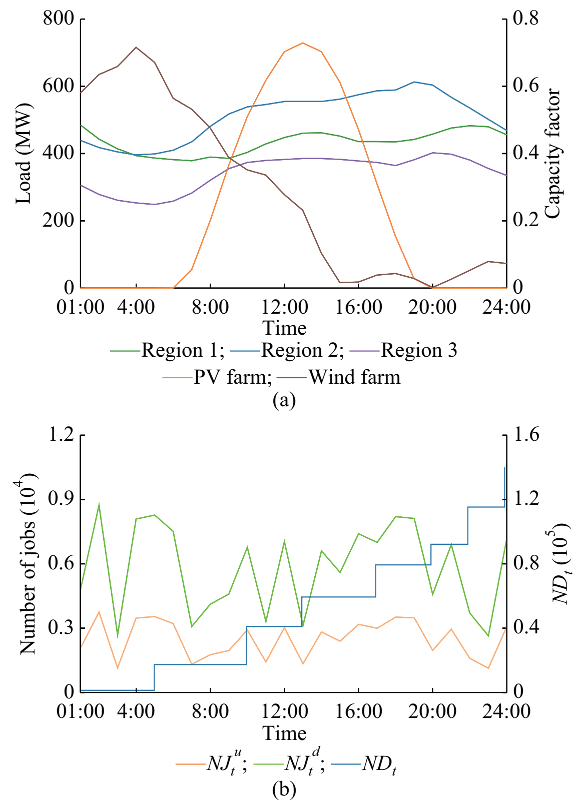

Fig. 3. Regional load profiles and capacity factor of RESs, numbers of non-deferrable and deferrable jobs, and minimum accumulated number of computational deferrable jobs. (a) Regional load profiles and capacity factor of RESs. (b) Numbers of non-deferrable and deferrable jobs and minimum accumulated number of computational deferrable jobs.

2) Scenarios

Traditionally, the reserve requirements are mainly met by conventional thermal units and energy storage. However, as this paper proposes, the reserves could also be supplied by data centers and cross-region systems. To evaluate the performance of the reserve provision from data centers and cross-region systems, we structure the following three scenarios.

1) Scenario S0 (denoted as BAU): without considering reserves supplied by data centers and cross-region systems.

2) Scenario S1 (denoted as DC_Res): considering reserves supplied by data centers, while cross-region reserve is not considered.

3) Scenario S2 (denoted as DCCR_Res): considering reserves supplied by both data centers and cross-region systems.

B. Simulation Results

1) Regional Upward Reserve

The supply composition and demand of regional upward reserves are shown in Fig. 4, where "(in)" and "(out)" represent imported and exported reserves, respectively. The reserve demand is defined as the reserve requirements from power loads minus the reserve provided by RESs.

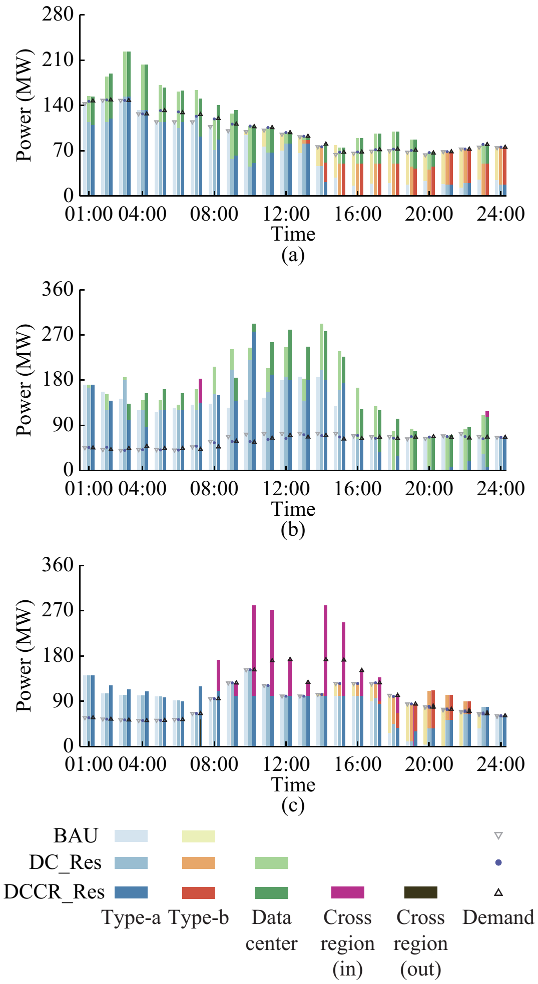

Fig. 4. Supply composition and demand of regional upward reserves. (a) Region 1. (b) Region 2. and (c) Region 3.

In Region 1, 73.4% and 26.6% of the upward reserves are supplied by type-a and type-b thermal units in the BAU, respectively. When considering the reserve supplied by data centers, the upward reserve supplied by thermal units decreases to 48.1% and 18.9% on average in the DC_Res and DCCR_Res, respectively. Meanwhile, the data centers in Region 1 contribute 32.9% of the upward reserve. The upward reserve demand in Region 1 in the DC_Res and DCCR_Res averagely increases by 4.8% compared with that in the BAU.

In Region 2, the upward reserve is completely supplied by type-a thermal units in the BAU. The proportion decreases to 68.4% and 66.9% in the DC_Res and DCCR_Res, respectively. Meanwhile, the data center could supply 31.6% of the upward reserve on average. In the DCCR_Res, 49.3% of available upward reserve in Region 2 is transmitted to Region 3 as cross-region reserve supply. Unlike Region 1, the upward reserve demand of Region 2 in the DC_Res and DCCR_Res decreases by 4.6% compared with that in the BAU.

In Region 3, the supply composition and demand of upward reserve remain nearly unchanged in the BAU and DC_Res. The upward reserve supplied by type-a and type-b thermal units accounts for 82.6% and 17.4%, respectively. The proportion decreases to 63.3% and 7.1% in the DCCR_Res, respectively, with Region 2 providing 29.6% of upward reserve. Especially during the periods from 09:00 to 11:00 and 13:00 to 15:00, the cross-region upward reserve exceeds 146.8% of that of local reserve. A higher upward reserve demand occurs in the DCCR_Res during the period from 10:00 to 16:00 due to the increased proportion of consumed RESs.

2) Data Center Dispatch

Figure 5 presents the migration of deferrable jobs between data centers in Regions 1 and 2 in the BAU and DC_Res. The deferrable job dispatch of data centers in Region 1 in the BAU and DC_Res is shown in Fig. 6. The migration and dispatch results of deferrable jobs are similar in the DC_Res and DCCR_Res, as both of them consider the reserve supplied by the data centers.

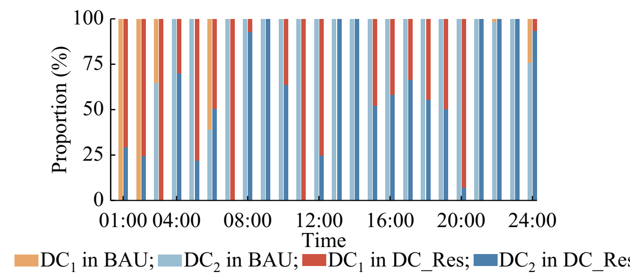

Fig. 5. Migration of deferrable jobs between data centers in Regions 1 and 2 in BAU and DC_Res.

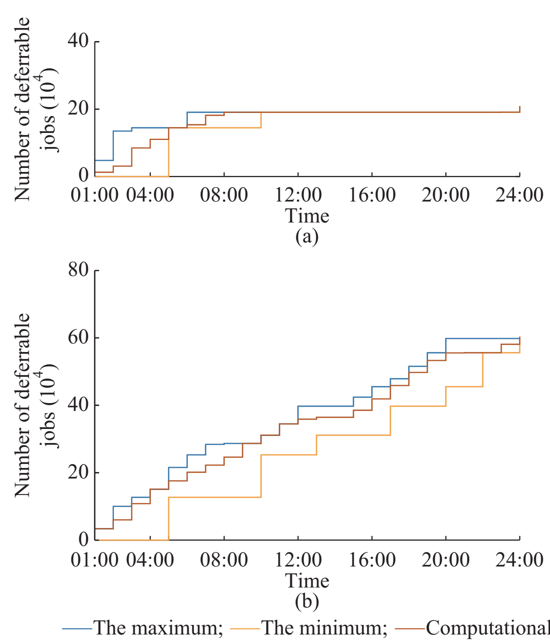

Fig. 6. Deferrable job dispatch of data centers in Region 1 in BAU and DC_Res. (a) BAU. (b) DC_Res.

The deferrable jobs are almost computed by the data centers in Region 2 in the BAU. Especially during the period from 06: 00 to 21: 00, the proportion of deferrable jobs distributed to the data centers in Region 2 remains 100%. In the DC_Res, however, several deferrable jobs are migrated to the data centers in Region 1. During the period from 14: 00 to 20: 00, the ratio of migrated deferrable jobs reaches 49.1%. Meanwhile, all the deferrable jobs are migrated from data centers in Region 2 to those in Region 1 during the periods from 06: 00 to 07: 00 and 10: 00 to 11: 00. Generally, 43.1% of the deferrable jobs are computed in Region 2 in the DC_Res, which is 2.9 times that in the BAU.

In the BAU, the accumulated computational job curve in Region 1 coincides with the curves of both the minimum and maximum numbers of deferrable jobs that should be computed. However, most of the deferrable jobs are timely computed in the data centers in Region 1 in DC_Res, making the accumulated computational job curve approach the curve of the maximum number of deferrable jobs that should be computed. Therefore, large quantities of upward reserve could be supplied by data centers in Region 1.

3) Renewable Energy Curtailment

The hourly wind power curtailment between 02:00 and 09: 00 and the hourly PV power curtailment between 10:00 and 18:00 are presented in Fig. 7. Both wind and PV power curtailments are zero during other periods.

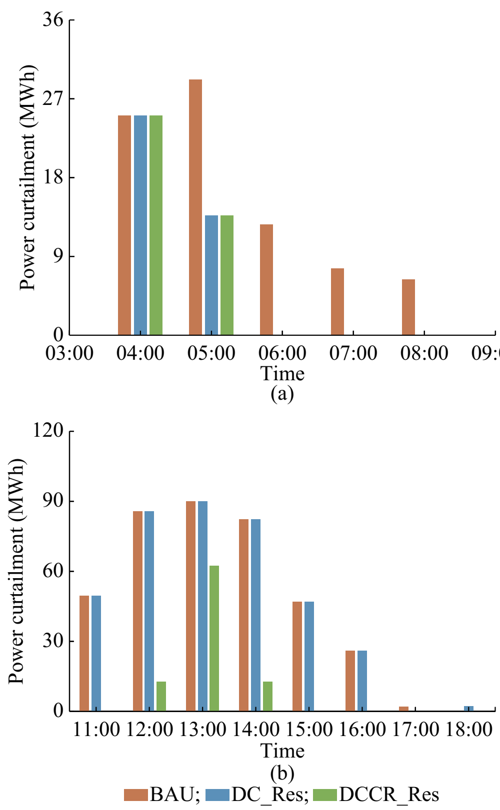

Fig. 7. Hourly wind and PV power curtailments. (a) Wind power curtailment. (b) PV power curtailment.

The wind power curtailment is the highest in the BAU, reaching the maximum value of 29.2 MWh during the period from 04:00 to 05:00. When considering the reserve supplied by data centers, more wind power could be consumed in the DC_Res and DCCR_Res. During the periods from 04: 00 to 05:00, the wind power curtailment in the DC_Res and DCCR_Res is 46.8% of that in the BAU. Especially during the periods from 05:00 to 06:00, 06:00 to 07:00, and 07:00 to 08: 00, the wind power curtailment drops to zero in the DC_Res and DCCR_Res, while it is 12.7, 7.6, and 6.4 MWh in the BAU, respectively.

In the BAU and DC_Res, the PV power curtailment is similar. The maximum PV power curtailment occurs during the period from 00:00 to 13:00, reaching 90.0 MWh. In the DCCR_Res, the test system shows the greatest ability to consume PV power. During the periods from 11:00 to 12:00, 12: 00 to 13:00, and 13:00 to 14:00, the PV power curtailment in the DCCR_Res decreases 85.2%, 30.6%, and 84.4% of that in the BAU (or DC_Res), respectively. Furthermore, no wind power curtailment occurs during the periods from 10: 00 to 11:00 and 14:00 to 18:00.

4) On/off Status of Type-b Thermal Units

Figure 8 shows the on/off status of type-b thermal units in Regions 1 and 3 in three scenarios. All the type-b thermal units in Region 2 remain off during the whole period.

In Region 1 in the BAU, one type-b thermal unit becomes on to provide both electricity and reserve from 09:00. Another type-b thermal unit starts up at 13:00. Both the two type-b thermal units remain on till 24:00. In the DC_Res and DCCR_Res, however, no type-b thermal unit is on during the period from 09: 00 to 12: 00, when the absent electricity would be supplied by type-a thermal units and the absent reserve would be provided by data centers.

In Region 3, one type-b thermal unit starts up at 13: 00, and then another two type-b thermal units start to provide electricity and reserve from 16: 00 in the BAU. The three type-b thermal units remain on till 22: 00. Because fewer jobs are computed in the data centers in Region 2 in the DC_Res, more electricity could be transmitted from Region 2 to Region 3 through the tie line during the period from 16: 00 to 23: 00. The additional transmitted electricity compensates for part of the power generation of type-b thermal units in Region 3, reducing the number of type-b thermal units that are on during the periods from 16:00 to 17:00 and 20: 00 to 21: 00. Furthermore, the number of type-b thermal units that are on in Region 3 decreases during the period from 13: 00 to 18: 00 in the DCCR_Res compared with that in the DC_Res. The corresponding reserve reduction is compensated by Region 2 through the tie line.

5) System Operation

The operating cost, renewable energy curtailment, and power generation of type-a and type-b thermal units in the test system are listed in Table I.

The operational cost is reduced by 0.5% and 1.7% in the DC_Res and DCCR_Res compared with that in the BAU, respectively. Meanwhile, the renewable energy curtailment drops by 9.1% and 72.7%, respectively. The power generation of type-a thermal units is almost the same in the three scenarios. In the DC_Res, the power generation of type-b thermal units decreases by 14.3% compared with that in the BAU. An additional 11.9% decrease in the power generation is achieved in the DCCR_Res.

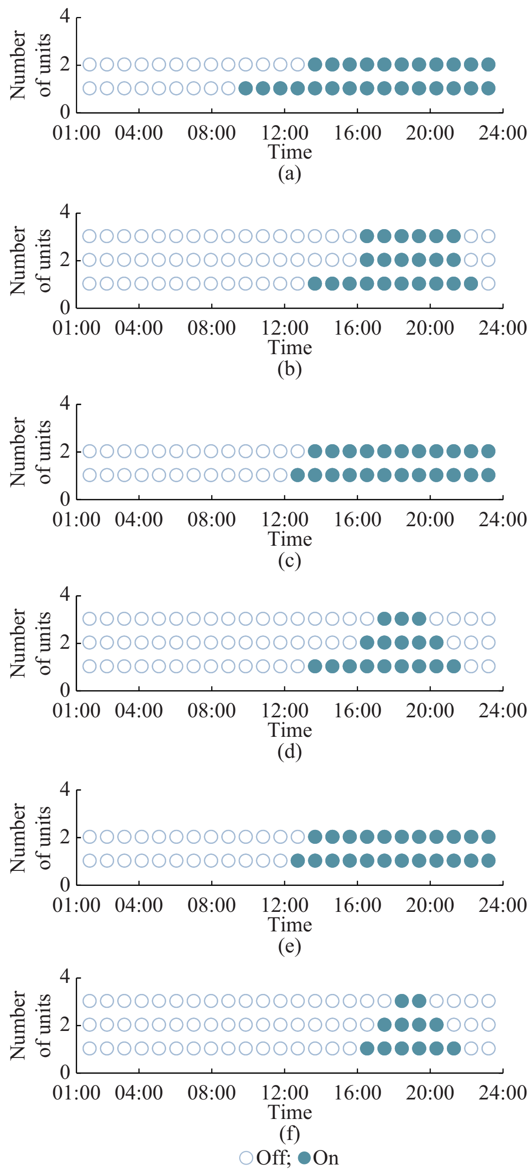

Fig. 8. On/off status of type-b thermal units in Regions 1 and 3 in three scenarios. (a) In Region 1 in BAU. (b) In Region 3 in BAU. (c) In Region 1 in DC_Res. (d) In Region 3 in DC_Res. (e) In Region 1 in DCCR_Res. (f) In Region 3 in DCCR_Res.

TABLE I
OPERATING COST, RENEWABLE ENERGY CURTAILMENT, AND POWER GENERATION OF TYPE-A AND TYPE-B THERMAL UNITS IN TEST SYSTEM

Scenario	Operating cost ($)	Renewable energy curtailment (MWh)	Power generation (GWh)	
			Type-a thermal unit	Type-b thermal unit
BAU	166400	463.5	27.7	983.9
DC_Res	165600	421.6	27.9	843.0
DCCR_Res	163500	126.7	27.7	743.0

C. Simulation on Eastern Inner Mongolia Power Grid System

To further validate the effectiveness and practicality of the reserve supply model for data centers, an additional case study is conducted based on the real-world eastern Inner Mongolia power grid system.

This system considers 45 thermal units with a total installed capacity of 18.1 GW, and the installed capacities of wind and PV reach 20.3 GW and 4.8 GW, respectively. In addition, energy storage, biomass generation, and hydropower are included, each contributing relatively small capacities compared with the dominant generation sources. The numbers of data center servers and jobs are scaled up to match the system load profile. In this simulation, data centers account for approximately 6.0% of the total electricity consumption.

Figure 9 presents the hourly power balance of the real-world eastern Inner Mongolia power grid system considering data centers in BAU and DC_Res, and Table II summarizes operating costs, renewable energy curtailments, power generations of thermal units, and CO_2 emissions.

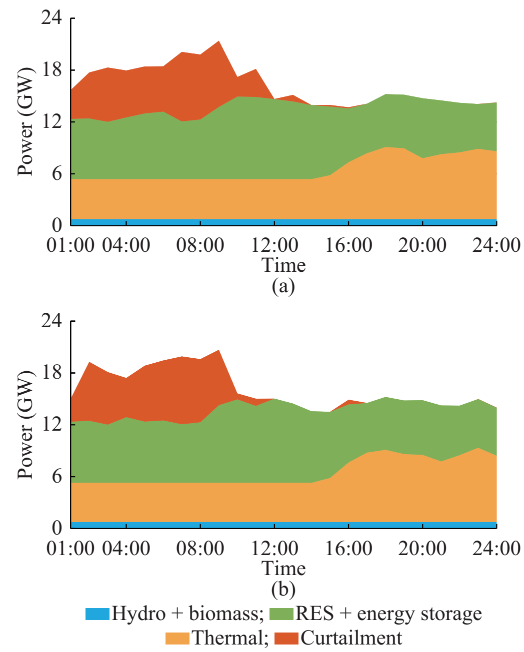

Fig. 9. Hourly power balance of real-world eastern Inner Mongolia power grid system considering data centers in BAU and DC_Res. (a) BAU. (b) DC_Res.

TABLE II
OPERATING COSTS, RENEWABLE ENERGY CURTAILMENTS, POWER GENERATIONS OF THERMAL UNITS, AND CO_2 EMISSIONS OF REAL-WORLD EASTERN INNER MONGOLIA POWER GRID SYSTEM

Scenario	Operating cost ($)	Renewable Energy curtailment (GWh)	Electricity generation (GWh)	CO_2 emission (kt)
BAU	3843100	34.5	138.9	114.6
DC_Res	3828000	33.9	138.4	114.4

Compared with the BAU, the DC_Res has shorter durations of renewable energy curtailment. The maximum hourly curtailed renewable energy generation decreases from 8.0 GWh to 7.8 GWh, and the total curtailed energy decreases from 34.5 GWh to 33.9 GWh. The power generation of thermal units drops by 0.5 GWh to 138.4 GWh, leading to a 0.2

kt reduction in CO_2 emissions. The operating cost decreases by 0.4%, reaching $3828000.

V. Conclusion

In this paper, we firstly propose the basic operational constraints of data centers and aggregate the computing constraints of various jobs. By analyzing the computing envelope for aggregated jobs, we formulate the available reserve capacity supplied by data centers. We then present the operating models of thermal units, energy storage, RESs, and regional power grid systems, as well as the objective function. The regional reserve constraints of multi-region system dispatch are emphasized, which consider both the local reserve demands and cross-region reserve supply. Finally, both a designed test system and a real-world power grid system are employed for simulation.

Notable benefits could be produced through utilizing reserves from data centers and cross-region systems. The dispatch of computational jobs among geo-distributed data centers and the composition of regional reserve supply have significant changes. The extreme concentration of deferrable jobs among multiple data centers is mitigated. Meanwhile, the deferrable jobs tend to be computed timely to provide upward reserves. Thermal units with high marginal costs operate for shorter periods, resulting in fewer reserve supply. The renewable energy integration is improved by 72.7% and 1.7%, along with a 1.7% and 0.4% reduction in operating costs, in the designed test system and the real-world power grid system, respectively.

In our future work, the uncertainty of computing requests, as well as the interdependencies between jobs, data locality issues, and job heterogeneity, will be incorporated to better reflect the operational realities of data centers. Meanwhile, the reserve supply capability of energy storage systems configured within data centers will also be investigated to further improve the operational flexibility of data centers.

References

[1] X. Wang and X. Cui. (2022, Jun.). Analysis of the power development and reform situation in China. [Online]. Available: http://www.chinacqpgx.com/hy/shownews?id=7887

[2] X. Chen, Y. Liu, Q. Wang *et al.*, "Path way toward carbon-neutral electrical systems in China by mid-century with negative CO_2 abatement costs informed by high-resolution modeling," *Joule*, vol. 5, no. 10, pp. 2715-2741, Oct. 2021.

[3] National Energy Administration. (2024, Jan.). National electricity industry statistics for 2023. [Online]. Available: https://www.nea.gov.cn/2024-01/26/c_1310762246.htm

[4] A. Berrada and K. Loudiyi, *Gravity Energy Storage*. Amsterdam: Elsevier, 2019, pp. 1-23.

[5] Y. Xu, C. Wan, H. Liu *et al.*, "Probabilistic forecasting-based reserve determination considering multi-temporal uncertainty of renewable energy generation," *IEEE Transactions on Power Systems*, vol. 39, no. 1, pp. 1019-1031, Jan. 2024.

[6] M. Cao and J. Yu, "Dynamic setting method of assessment indicators for power curves of renewable energy sources considering scarcity of reserve resources," *Journal of Modern Power Systems and Clean Energy*, vol. 12, no. 1, pp. 101-114, Jan. 2024.

[7] M. Chen, C. Gao, M. Song *et al.*, "Internet data centers participating in demand response: a comprehensive review," *Renewable and Sustainable Energy Reviews*, vol. 117, p. 109466, Jan. 2020.

[8] B. Zou, G. Chen, H. Zhang *et al.*, "Coordinating multiple geo-distributed data centers for enhanced participation in frequency regulation services under uncertainty," *Journal of Modern Power Systems and Clean Energy*, vol. 13, no. 5, pp. 1677-1688, Sept. 2025.

[9] Z. Dong. (2023, Oct.). Data centers and electricity synergy for sustainable development. [Online]. Available: http://paper.people.com.cn/zgnyb/html/2023-10/16/content_26022894.htm

[10] T. Wan, Y. Tao, J. Qiu *et al.*, "Internet data centers participating in electricity network transition considering carbon-oriented demand response," *Applied Energy*, vol. 329, p. 120305, Jan. 2023.

[11] M. Chen, C. Gao, M. Shahidehpour *et al.*, "Internet data center load modeling for demand response considering the coupling of multiple regulation methods," *IEEE Transactions on Smart Grid*, vol. 12, no. 3, pp. 2060-2076, May 2021.

[12] K. Taghizad-Tavana, M. Tarafdar-Hagh, S. Nojavan *et al.*, "Operation of smart distribution networks by considering the spatial-temporal flexibility of data centers and battery energy storage systems," *Sustainable Cities and Society*, vol. 114, p. 105746, Nov. 2024.

[13] C. Jiang, C. L. Tseng, Y. Wang *et al.*, "Optimal pricing strategy for data center considering demand response and renewable energy source accommodation," *Journal of Modern Power Systems and Clean Energy*, vol. 11, no. 1, pp. 345-354, Jan. 2023.

[14] Y. Zhang, D. C. Wilson, I. C. Paschalidis *et al.*, "HPC data center participation in demand response: an adaptive policy with QoS assurance," *IEEE Transactions on Sustainable Computing*, vol. 7, no. 1, pp. 157-171, Jan. 2022.

[15] Y. Fu, X. Han, K. Baker *et al.*, "Assessments of data centers for provision of frequency regulation," *Applied Energy*, vol. 277, p. 115621, Nov. 2020.

[16] D. A. Kez, A. M. Foley, S. M. Muyeen *et al.*, "Manipulation of static and dynamic data center power responses to support grid operations," *IEEE Access*, vol. 8, pp. 182078-182091, Oct. 2020.

[17] M. Chen, C. Gao, Z. Li *et al.*, "Aggregated model of data network for the provision of demand response in generation and transmission expansion planning," *IEEE Transactions on Smart Grid*, vol. 12, no. 1, pp. 512-523, Jan. 2021.

[18] L. Cupelli, N. Barve, and A. Monti, "Optimal sizing of data center battery energy storage system for provision of frequency containment reserve," in *Proceedings of 43rd Annual Conference of the IEEE Industrial Electronics Society*, Beijing, China, Oct.-Nov. 2017, pp. 7185-7190.

[19] H. Chen, B. Zhang, M. C. Caramanis *et al.*, "Data center optimal regulation service reserve provision with explicit modeling of quality of service dynamics," in *Proceedings of 2015 54th IEEE Conference on Decision and Control*, Osaka, Japan, Dec. 2015, pp. 7207-7213.

[20] H. Chen, Y. Zhang, M. C. Caramanis *et al.*, "EnergyQARE: QoS-aware data center participation in smart grid regulation service reserve provision," *ACM Transactions on Modeling and Performance Evaluation of Computing Systems*, vol. 4, no. 1, pp. 1-31, Mar. 2019.

[21] L. Ma, H. Hui, S. Wang *et al.*, "Coordinated optimization of power-communication coupling networks for dispatching large-scale flexible loads to provide operating reserve," *Applied Energy*, vol. 359, p. 122705, Apr. 2024.

[22] M. Zare, M. R. Narimani, M. Malekpour *et al.*, "Reserve constrained dynamic economic dispatch in multi-area power systems: an improved fireworks algorithm," *International Journal of Electrical Power & Energy Systems*, vol. 126, p. 106579, Mar. 2021.

[23] G. Wu, Y. Xiang, J. Liu *et al.*, "Decentralized day-ahead scheduling of multi-area integrated electricity and natural gas systems considering reserve optimization," *Energy*, vol. 198, p. 117271, May 2020.

[24] L. He, Z. Lu, J. Zhang *et al.*, "Economic dispatch of multi-area integrated electricity and natural gas systems considering emission and hourly spinning reserve constraints," *International Journal of Electrical Power & Energy Systems*, vol. 132, p. 107177, Nov. 2021.

[25] J. B. Mogo and I. Kamwa, "Improved deterministic reserve allocation method for multi-area unit scheduling and dispatch under wind uncertainty," *Journal of Modern Power Systems and Clean Energy*, vol. 7, no. 5, pp. 1142-1154, Sept. 2019.

[26] L. Xiang, S. Shao, J. Wu *et al.*, "A fully distributed optimization method for reserve capacity of multi-area interconnected power systems considering reserve sharing," in *Proceedings of 2021 40th Chinese Control Conference*, Shanghai, China, Jul. 2021, pp. 1785-1790.

[27] M. Zhou, M. Wang, J. Li *et al.*, "Multi-area generation-reserve joint dispatch approach considering wind power cross-regional accommodation," *CSEE Journal of Power and Energy Systems*, vol. 3, no. 1, pp. 74-83, Mar. 2017.

[28] M. Wang, M. Zhou, H. Bai *et al.*, "A generation-reserve co-optimization approach considering wind power cross-regional accommodation," in *Proceedings of 2015 5th International Conference on Electric Utility Deregulation and Restructuring and Power Technologies*,

Changsha, China, Nov. 2016, pp. 620-625.
[29] A. Papavasiliou, A. Bouso, S. Apelfrojd *et al*., "Multi-area reserve dimensioning using chance-constrained optimization," *IEEE Transactions on Power Systems*, vol. 37, no. 5, pp. 3982-3994, Sept. 2022.
[30] J. Xu, S. Liao, H. Jiang *et al*., "A multi-time scale tie-line energy and reserve allocation model considering wind power uncertainties for multi-area systems," *CSEE Journal of Power and Energy Systems*, vol. 7, no. 4, pp. 677-687, Jul. 2021.
[31] L. Wang, H. Jiang, and Y. Jiang, "A multi-time scale Tie-line energy and reserve allocation model considering wind power uncertainty for multi-area system in hierarchical control structure," in *Proceedings of 2021 IEEE International Conference on Emergency Science and Information Technology*, Chongqing, China, Nov. 2022, pp. 139-149.
[32] H. Jiang, J. Xu, Y. Sun *et al*., "Dynamic reserve demand estimation model and cost-effectivity oriented reserve allocation strategy for multi-area system integrated with wind power," *IET Generation, Transmission & Distribution*, vol. 12, no. 7, pp. 1606-1620, Apr. 2018.
[33] T. Jin, L. Bai, M. Yan *et al*., "Unlocking spatio-temporal flexibility of data centers in multiple regional peer-to-peer energy transaction markets," *IEEE Transactions on Power Systems*, vol. 40, no. 5, pp. 3914-3927, Sept. 2025.
[34] Entsoe. (2023, May). Transparency platform. [Online]. Available: https://transparency.entsoe.eu
[35] T. Jin, X. Chen, J. Wen *et al*., "Improved ramping and reserve modeling of combined heat and power in integrated energy systems for better renewable integration," *IEEE Transactions on Sustainable Energy*, vol. 13, no. 2, pp. 683-692, Apr. 2022.
[36] Y. Li, X. Long, C. Zhou *et al*., "Coordinated operations of highly renewable power systems and distributed data centers," *Scientia Sinica Technologica*, vol. 54, no. 1, pp. 119-135, Jan. 2024.

Tianyu Jin received the B.S. and Ph.D. degrees in electrical engineering from Huazhong University of Science and Technology, Wuhan, China, in 2020 and 2025, respectively. From 2023 to 2024, he was a Visiting Scholar with the University of North Carolina at Charlotte, Charlotte, USA. His research interests include integrated energy system, data center dispatch, and peer-to-peer energy trading.

Yuke Lu is with the Institute of New Energy, Wuhan, China. His research interests include power system operation and optimization and electricity market.

Linquan Bai received the B.S. and M.S. degrees in electrical engineering from Tianjin University, Tianjin, China, in 2010 and 2013, respectively, and the Ph.D. degree in electrical engineering from the University of Tennessee, Knoxville, USA, in 2017. He is an Adjunct Research Professor with the University of North Carolina at Charlotte, Charlotte, USA. He is an Associate Editor of IEEE Transactions on Sustainable Energy, IEEE Power Engineering Letters, and Journal of Modern Power System and Clean Energy. His research interests include grid integration of distributed energy resource, power system optimization, and electricity market.

Xinyu Chen received the B.S. and Ph.D. degrees in electrical engineering from Tsinghua University, Beijing, China, in 2009 and 2014, respectively. He was an exchange Ph.D. student with Harvard University, Cambridge, USA, in 2012. He hosted positions of Post-doctoral Researcher and Lecturer at Harvard University from 2015 to 2019. He is currently a Professor at Huazhong University of Science and Technology, Wuhan, China. His research interests include power system operation and planning, multi-energy system optimization, renewable energy integration, and energy policy.

Jinyu Wen received the B.Eng. and Ph.D. degrees all in electrical engineering from the Huazhong University of Science and Technology (HUST), Wuhan, China, in 1992 and 1998, respectively. He was a Visiting Student from 1996 to 1997 and a Research Fellow from 2002 to 2003 all with the University of Liverpool, Liverpool, U.K., and a Senior Visiting Researcher with the University of Texas at Arlington, Arlington, USA, in 2010. From 1998 to 2002, he was a Director Engineer in XJ Electric Company Ltd., Xuchang, China. In 2003, he joined the HUST and currently is a Professor with HUST. His current research interests include renewable energy integration, energy storage application, DC grid, and power system operation and control.

Yuxin Zhang received the B.S. degree in electrical engineering from Huazhong University of Science and Technology (HUST), Wuhan, China, in 2020. He is currently pursuing the Ph.D. degree in electrical engineering with HUST. His research interests include electricity market and carbon market.